# Molecular Threading and Tunable Molecular Recognition on DNA Origami Nanostructures

Na Wu,[†,#] Daniel M. Czajkowsky,[‡,#] Jinjin Zhang,[†] Jianxun Qu,[‡] Ming Ye,[†] Dongdong Zeng,[†] Xingfei Zhou,[§] Jun Hu,*[,†] Zhifeng Shao,[‡] Bin Li,*[,†] and Chunhai Fan*[,†]

[†]Division of Physical Biology, and Bioimaging Center, Shanghai Synchrotron Radiation Facility, Shanghai Institute of Applied Physics, Chinese Academy of Sciences, Shanghai 201800, China
[‡]School of Biomedical Engineering, Shanghai Jiao Tong University, Shanghai 200240, China
[§]Physics Department, Ningbo University, Zhejiang 315211, China

**S** *Supporting Information*

**ABSTRACT:** The DNA origami technology holds great promise for the assembly of nanoscopic technological devices and studies of biochemical reactions at the single-molecule level. For these, it is essential to establish well controlled attachment of functional materials to predefined sites on the DNA origami nanostructures for reliable measurements and versatile applications. However, the two-sided nature of the origami scaffold has shown limitations in this regard. We hypothesized that holes of the commonly used two-dimensional DNA origami designs are large enough for the passage of single-stranded (ss)-DNA. Sufficiently long ssDNA initially located on one side of the origami should thus be able to "thread" to the other side through the holes in the origami sheet. By using an origami sheet attached with patterned biotinylated ssDNA spacers and monitoring streptavidin binding with atomic force microscopic (AFM) imaging, we provide unambiguous evidence that the biotin ligands positioned on one side have indeed threaded through to the other side. Our finding reveals a previously overlooked critical design feature that should provide new interpretations to previous experiments and new opportunities for the construction of origami structures with new functional capabilities.

DNA origami, in which a long strand of single-stranded (ss)-DNA is folded into specific shapes by a large number of shorter "staple" ss-DNA strands, can form a wide variety of two- or three-dimensional structures with nanoscale precision.[1–3] Moreover, the ends of the staple strands can be modified to contain ligands (such as biotin or additional ssDNA) for complex formation with functional materials such as gold nanoparticles, carbon nanotubes, or proteins.[4–8] There is thus tremendous promise of this material as scaffolds for the controlled assembly of nanostructures for many chemical, biophysical, or technological applications. Of particular note with the latter, the top-down lithographic fabrication on technologically useful materials (such as $SiO_2$ and diamond-like carbon) recently facilitated the location-specific adsorption of 2D origami onto these materials.[9,10] Combined with a bottom-up assembly of nanostructures on the origami, such position-specific adsorption allows for a potentially significant reduction in the size of electrical or optical devices.

However there are still significant technical hurdles that must be overcome with this assembly strategy. One of the most challenging stems from the two-sided nature of the 2D origami: adsorption to the substrate can occur by either side of the scaffold.[11] As a result, some of the adsorbed origami will be oriented with their ligands facing the solid surface, inaccessible to their binding partners in solution, resulting in non-functionalized scaffolds. This is a widely observed characteristic in many studies using 2D origami.[5,12–15] With some origami designs, the fraction of such "face-down" origami is approximately half (as might be expected),[1] although fractions lower than half have also been noted with other designs.[14] While the reasons of these differences are not presently known, any sizable fraction of nonfunctionalized origami is, for technological applications in particular, an unacceptable design feature that fundamentally prohibits further development of this technology.

As a material, 2D DNA origami is a lattice of hybridized double-stranded (ds)-DNA segments interspersed with holes.[1,16,17] While much effort has focused on designing novel dsDNA connections for the production of unique shapes and structures, the holes, to our knowledge, have heretofore not been explored for their practical utility. We reasoned that the sizes of the holes in the commonly used 2D origami sheets could be large enough to enable the passage of suitably small ligands and spacers, if the spacers were sufficiently long. Hence, for surface-adsorbed origami, the ligands originally on the surface-facing side of the sheet might transiently pass (or "thread") through these holes as a result of simple thermal fluctuations. The transient presence of the ligands on the solution-facing side of the origami would then enable binding to the desired nanoscopic component in the solution. In this way, whether the origami is oriented with the ligand/spacer attachment sites facing the substrate or the solution, all of the components could bind to all of the adsorbed origami.

To provide some measure of the shape, size, and structural variations of these holes, we first employed all-atom molecular dynamics (MD) simulations of a 2D origami sheet (Figure 1).
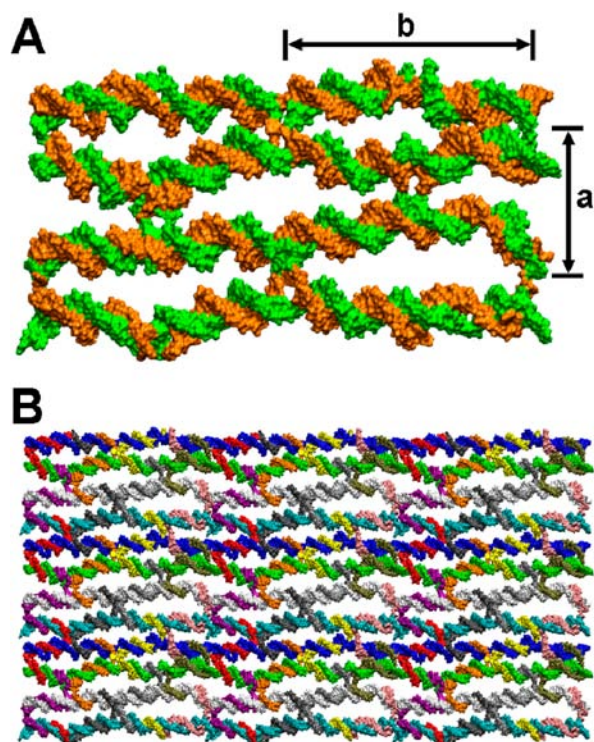
**Figure 1.** MD simulations of the 2D origami. (A) Snapshot of a unit cell of the simulated 4-stranded B-DNA assembly. The lattice dimensions (**a** and **b**) are indicated. (B) The interstrand connections are the same as those of the origami sheet experimentally investigated.
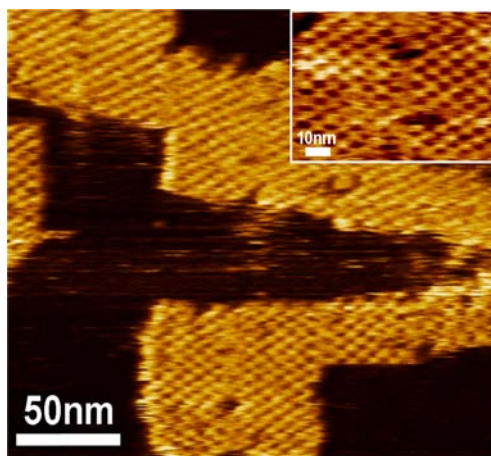


**Figure 2.** FM-AFM image of the origami blocks on mica under solution. The inset shows the rectangular brick-like pattern of the block at a higher resolution.

We investigated a 4-stranded B-DNA assembly connected to its periodic image so that effectively an infinitely large origami sheet, consisting of periodic arrays of this 4-stranded assembly, was evaluated. Obtaining measurements from a 10 ns trajectory after the system had equilibrated, we found that the lattice dimensions are **a** = 5.7 ± 0.3 nm and **b** = 10.5 ± 0.2 nm (see Figure 1 for definitions and Supporting Information for further details). These dimensions correspond to a hole size of 1.7 ± 0.3 nm and 8.5 ± 0.2 nm along the **a**- and **b**-directions, respectively (assuming 4 and 2 nm of DNA along the **a**- and **b**-directions, respectively). However, direct inspection of the holes in these simulations reveals that they are somewhat elliptical and fluctuate in size and shape. For the duration of the simulation, however, the central ∼3 nm along the **b**-direction exhibits lengths of between ∼1.3 to 1.7 nm along the **a**-direction (see Supporting Information for further details).

We verified these measurements by obtaining direct images of individual origami sheets with frequency modulation-atomic force microscopy (FM-AFM).[16] Rectangular origami similar to those employed in the simulations were adsorbed onto mica and imaged under buffer solution. As shown in Figure 2, the substructure of the origami sheets is well-resolved in these images, showing the sheet to consist of a rectangular brick-like array of protrusions with lattice dimensions of **a** = 5.1 ± 0.3 nm and **b** = 9.2 ± 0.4 nm, similar to the results from the MD simulations. The variation in the distances between adjacent protrusions (and also the holes) is thus rather small. The slight differences in lengths compared to the simulations may be owing to the absence of polarization terms in the force field.[18] Calculated as above, these dimensions correspond to hole sizes of 1.1 ± 0.3 nm and 7.2 ± 0.4 nm along the **a**- and **b**-directions, respectively. Also, assuming a similar oval shape for the hole,

the central ∼3 nm along the **b**-direction would exhibit lengths of between ∼0.8 to 1.1 nm along the **a**-direction based on these FM-AFM measurements. We should note that a similar hole size was recently observed in a cryoelectron microscopy study of a 3D origami structure that exhibits a similar hybridization pattern as in the 2D origami studied here.[19]

Taken together, these results indicate that the holes in this origami should be sufficiently large to accommodate spacers whose cross-section is at least roughly 1 × 3 nm². In a completely extended form, the cross-section of ssDNA is ∼0.8 × 1 nm², well within this hole dimension. Moreover, biotin is a cylindrical molecule, approximately 0.6 nm in diameter and 1.2 nm long,[20] also smaller than this hole size. Further, calculations of the free energy associated with ssDNA translocation through these holes indicate an energy barrier of less than ∼2kT, which would be easily overcome with thermal fluctuations (Figure S2, Supporting Information). We thus expected that biotinylated ssDNA should prove a generally useful threading agent for this commonly used 2D DNA origami design.

To test this, we evaluated the ability of streptavidin (SA) to bind to substrate-adsorbed origami with several biotinylated ssDNA positioned at specific locations within the origami sheet (Figure 3). The locations of the labels enable an unambiguous
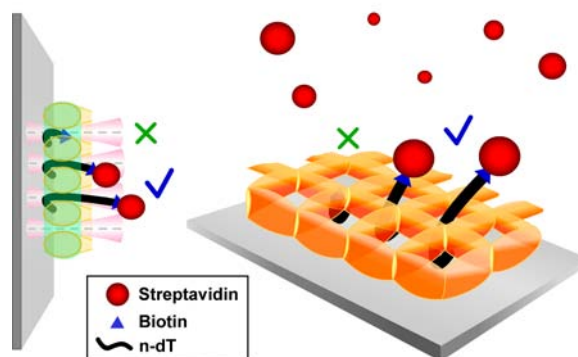


**Figure 3.** Schematic diagram of the proposed molecular threading mechanism. Spacers that are sufficiently long transiently tunnel through the holes in the origami block where they can bind to the SA in solution.

identification of the origami orientation on the mica surface. Individual binding events of SA to these origami were observed using time-lapse AFM,[21] by which samples are continuously imaged by tapping mode AFM after the addition of SA until equilibrium binding is achieved, so that the rate and extent of binding events can both be determined in these measurements.

We first evaluated the case in which the biotin labels are attached directly to the ends of the staple strands (that is, without any ssDNA spacer, termed 0-dT). As shown in Figure 4a, there are two different populations of origami: those with
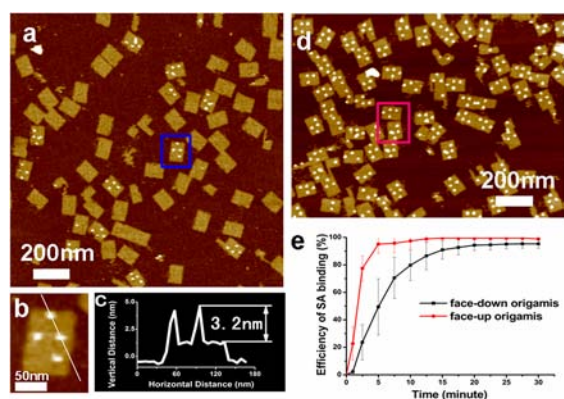


**Figure 4.** Evaluation of SA-biotin binding reactions on origami with and without spacers by time-lapse AFM. (a) Without spacers (0-dT-biotin). (b) Magnified region within the blue rectangle in (a). (c) Cross-sectional height profile along the white line in (b). (d) Origami with a 5-dT spacer. The pink rectangle shows two patterns, one consistent with a face-up orientation and one with a face-down orientation. (e) SA binding dynamics.

1−4 (most frequently 4) bright spots on their surface and those without any bright spots. The bright spots are the expected size of individual SA molecules in these images (Figure 4b,c),[21,22] and so their positions identify the locations of accessible biotin ligands in the adsorbed sheet. For those origami with four SA bound, their distribution on each origami was identical, namely that expected for origami with the ligand attachment points facing the solution ("face-up" origami). Hence, these results suggest that there may be two different orientations of the adsorbed origami sheets: face-up origami with biotin labels accessible to SA binding and face-down origami with biotin labels facing the mica substrate and inaccessible to SA. We note that the observation of the face-up pattern in this case confirms a proper localization of the ligands in the 2D sheet, an issue of previous concern.[15]

For the samples with ssDNA spacer lengths of 5-dT, the images following SA addition were markedly different than those in the 0-dT case: all of the origami surfaces now contained 1−4 bright spots of the expected size of SA (Figure 4d). For the origami with four SA bound, there were two different populations based on the SA patterns: those consistent with the face-up origami and those consistent with the face-down pattern (see the pink rectangle in Figure 4d for a region showing origami sheets with each of these chiral patterns). Detection of the face-down pattern in this case demonstrates that even though the origami are oriented with the biotinylated ssDNA attachment points facing the mica, the biotin ligands are nonetheless accessible to the SA in solution. Hence, with a spacer length of 5-dT, the biotinylated ligands have indeed threaded through the holes in the adsorbed

origami and become accessible to SA in the solution. We note that the maximal extension of this ssDNA spacer is expected to be ∼3.2 nm (with ∼6.3 Å per base),[23] sufficiently larger than the ∼2 nm thickness of the origami sheet, although it is more likely that the ssDNA, away from the hole, is in a more compact configuration.[23,24]

We found that although the spacer length is the same, the rate at which SA bound to the face-up or face-down origami sheets is different, with binding occurring more slowly to the face-down origami (Figure 4e). A reduced rate of binding to the face-down origami could be owing to sterically inhibited access as a result of an effectively shorter length of the spacer projecting out of the origami in the face-down orientation compared with that in the face-up orientation (because of the thickness of the origami sheet).[25] Such a steric inhibition could also have contributed to the results observed in the 0-dT case. This suggests that there should be a dependence of the rate of SA binding to face-down origami on spacer length, as there should also be in fact with the proposed threading mechanism. We thus evaluated the rates of SA binding over a range of spacer lengths and indeed observed a striking increase of binding rate with an increasing spacer length for the face-down origami (Figure 5). A set of AFM images showing the time
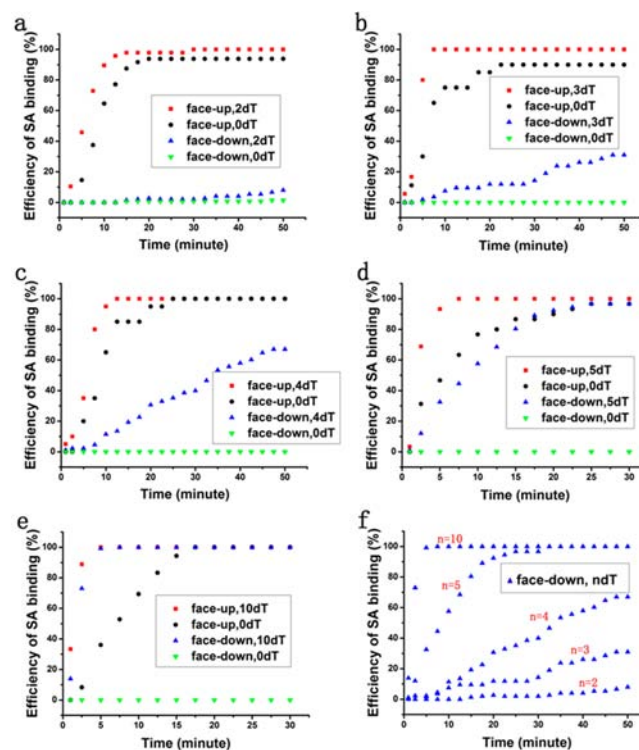


**Figure 5.** SA-biotin binding dynamics as a function of a spacer length (n-dT). Shown are the time dependent changes in binding efficiency with spacer lengths from $n = 0$ to $n = 10$.

evolution of this binding process is shown in Figure S4 (Supporting Information). There is also a slight dependence of SA binding to face-up origami, quicker at longer linker lengths (Figure 5a−e), perhaps also owing to the steric effects mentioned above for the face-down origami. Hence, not only do these results provide additional support for the proposed threading process, but also they demonstrate that, for a maximal binding rate and extent to these origami, whether face-up or face-down, a spacer length of at least 10-dT is most effective.

We note that slightly longer spacer lengths (15-dT and 20-dT) yielded similar binding rates as in the 10-dT case, with only slight differences in efficiency (Figure S6, Supporting Information).

Thus, we have identified molecular threading as a means by which all surface bound origami can become maximally bound by nanosized molecular complexes. Our results suggest that any ligand/spacer that is smaller than $1 \times 3$ nm$^2$ should be able to thread though the origami sheet, which should be easily implemented in strategies for technological applications. Threading would also enable an increase in the density of addressable features that are possible on a single origami face, without lowering origami stability. Conversely, ligands or spacers larger than the hole dimensions would prevent threading, which is also a desired feature in certain applications. In particular, the common use of additional ssDNA as "sticky ends" to form the nanostructures on the origami is probably complicated as a result of the threading described here.[4,12,26,27] Overall, the holes in the origami lattice should now be recognized as a design feature that can both affect experimental outcome and provide new opportunities for the production of novel origami structures and functional abilities.

## ■ ASSOCIATED CONTENT

### Ⓢ Supporting Information

Experimental section and additional data. This material is available free of charge via the Internet at http://pubs.acs.org.

## ■ AUTHOR INFORMATION

### Corresponding Author

libin@sinap.ac.cn; fchh@sinap.ac.cn; hujun@sinap.ac.cn

### Author Contributions

#N. Wu and D. M. Czajkowsky contributed equally.

### Notes

The authors declare no competing financial interest.

## ■ ACKNOWLEDGMENTS

## ■ REFERENCES

(1) Rothemund, P. W. K. *Nature* **2006**, *440*, 297.
(2) Torring, T.; Voigt, N. V.; Nangreave, J.; Yan, H.; Gothelf, K. V. *Chem. Soc. Rev.* **2011**, *40*, 5636.
(3) Saccà, B.; Niemeyer, C. M. *Angew. Chem., Int. Ed.* **2012**, *51*, 58.
(4) Ding, B. Q.; Deng, Z. T.; Yan, H.; Cabrini, S.; Zuckermann, R. N.; Bokor, J. *J. Am. Chem. Soc.* **2010**, *132*, 3248.
(5) Voigt, N. V.; Torring, T.; Rotaru, A.; Jacobsen, M. F.; Ravnsbaek, J. B.; Subramani, R.; Mamdouh, W.; Kjems, J.; Mokhir, A.; Besenbacher, F.; Gothelf, K. V. *Nat. Nanotechnol.* **2010**, *5*, 200.
(6) Pal, S.; Deng, Z. T.; Ding, B. Q.; Yan, H.; Liu, Y. *Angew. Chem., Int. Ed.* **2010**, *49*, 2700.
(7) Pearson, A. C.; Liu, J.; Pound, E.; Uprety, B.; Woolley, A. T.; Davis, R. C.; Harb, J. N. *J. Phys. Chem. B* **2012**, *116*, 10551.
(8) Rajendran, A.; Endo, M.; Sugiyama, H. *Angew. Chem., Int. Ed.* **2012**, *51*, 874.
(9) Kershner, R. J.; Bozano, L. D.; Micheel, C. M.; Hung, A. M.; Fornof, A. R.; Cha, J. N.; Rettner, C. T.; Bersani, M.; Frommer, J.; Rothemund, P. W. K.; Wallraff, G. M. *Nat. Nanotechnol.* **2009**, *4*, 557.
(10) Hung, A. M.; Micheel, C. M.; Bozano, L. D.; Osterbur, L. W.; Wallraff, G. M.; Cha, J. N. *Nat. Nanotechnol.* **2010**, *5*, 121.
(11) Kim, K. N.; Sarveswaran, K.; Mark, L.; Lieberman, M. *Soft Matter* **2011**, *7*, 4636.
(12) Lund, K.; Manzo, A. J.; Dabby, N.; Michelotti, N.; Johnson-Buck, A.; Nangreave, J.; Taylor, S.; Pei, R. J.; Stojanovic, M. N.; Walter, N. G.; Winfree, E.; Yan, H. *Nature* **2010**, *465*, 206.
(13) Wickham, S. F. J.; Endo, M.; Katsuda, Y.; Hidaka, K.; Bath, J.; Sugiyama, H.; Turberfield, A. J. *Nat. Nanotechnol.* **2011**, *6*, 166.
(14) Qian, L.; Wang, Y.; Zhang, Z.; Zhao, J.; Pan, D.; Zhang, Y.; Liu, Q.; Fan, C.; Hu, J.; He, L. *Chin. Sci. Bull.* **2006**, *51*, 2973.
(15) Sacca, B.; Meyer, R.; Erkelenz, M.; Kiko, K.; Arndt, A.; Schroeder, H.; Rabe, K. S.; Niemeyer, C. M. *Angew. Chem., Int. Ed.* **2010**, *49*, 9378.
(16) Yamada, H.; Kobayashi, K.; Fukuma, T.; Hirata, Y.; Kajita, T.; Matsushige, K. *Appl. Phys. Express* **2009**, *2*, 95007.
(17) Zhang, C.; He, Y.; Chen, Y.; Ribbe, A. E.; Mao, C. *J. Am. Chem. Soc.* **2007**, *129*, 14134.
(18) Babin, V.; Baucom, J.; Darden, T. A.; Sagui, C. *J. Phys. Chem. B* **2006**, *110*, 11571.
(19) Bai, X. C.; Martin, T. G.; Scheres, S. H. W.; Dietz, H. *Proc. Natl. Acad. Sci. U. S. A.* **2012**, *109*, 20012.
(20) Weber, P. C.; Ohlendorf, D.; Wendoloski, J.; Salemme, F. *Science* **1989**, *243*, 85.
(21) Wu, N.; Zhou, X. F.; Czajkowsky, D. M.; Ye, M.; Zeng, D. D.; Fu, Y. M.; Fan, C. H.; Hu, J.; Li, B. *Nanoscale* **2011**, *3*, 2481.
(22) Zhang, Z.; Wang, Y.; Fan, C. H.; Li, C.; Li, Y.; Qian, L. L.; Fu, Y. M.; Shi, Y. Y.; Hu, J.; He, L. *Adv. Mater.* **2010**, *22*, 2672.
(23) Murphy, M.; Rasnik, I.; Cheng, W.; Lohman, T. M.; Ha, T. *Biophys. J.* **2004**, *86*, 2530.
(24) Chen, H.; Meisburger, S. P.; Pabit, S. A.; Sutton, J. L.; Webb, W. W.; Pollack, L. *Proc. Natl. Acad. Sci. U. S. A.* **2012**, *109*, 799.
(25) Ko, S. H.; Gallatin, G. M.; Liddle, J. A. *Adv. Funct. Mater.* **2012**, *22*, 1015.
(26) Maune, H. T.; Han, S. P.; Barish, R. D.; Bockrath, M.; Goddard, W. A.; Rothemund, P. W. K.; Winfree, E. *Nat. Nanotechnol.* **2010**, *5*, 61.
(27) Kuzyk, A.; Schreiber, R.; Fan, Z.; Pardatscher, G.; Roller, E.-M.; Högele, A.; Simmel, F. C.; Govorov, A. O.; Liedl, T. *Nature* **2012**, *483*, 311.